



HAL
open science

Adherens junctions are involved in polarized contractile ring formation in dividing epithelial cells of *Xenopus laevis* embryos

Guillaume Hatte, Claude Prigent, Jean-Pierre Tassan

► **To cite this version:**

Guillaume Hatte, Claude Prigent, Jean-Pierre Tassan. Adherens junctions are involved in polarized contractile ring formation in dividing epithelial cells of *Xenopus laevis* embryos. *Experimental Cell Research*, 2021, 402 (1), pp.112525. 10.1016/j.yexcr.2021.112525 . hal-03169727

HAL Id: hal-03169727

<https://hal.science/hal-03169727>

Submitted on 29 Mar 2021

HAL is a multi-disciplinary open access archive for the deposit and dissemination of scientific research documents, whether they are published or not. The documents may come from teaching and research institutions in France or abroad, or from public or private research centers.

L'archive ouverte pluridisciplinaire **HAL**, est destinée au dépôt et à la diffusion de documents scientifiques de niveau recherche, publiés ou non, émanant des établissements d'enseignement et de recherche français ou étrangers, des laboratoires publics ou privés.

1 **Adherens junctions are involved in polarized contractile ring formation in**
2 **dividing epithelial cells of *Xenopus laevis* embryos**

3

4 Guillaume Hatte¹, Claude Prigent^{1,2} and Jean-Pierre Tassan^{1*}

5 1 : Univ Rennes, CNRS, IGDR (Institut de Génétique et Développement de Rennes),
6 UMR 6290, 2 Avenue du Professeur Leon Bernard, 35000 Rennes, France

7 2 : Present address starting January 1st, 2021 : Centre de Recherche de Biologie
8 cellulaire de Montpellier (CRBM), University of Montpellier, CNRS, 34293 Montpellier,
9 France.

10 * Corresponding author.

11 E-mail address : jean-pierre.tassan@univ-rennes1.fr

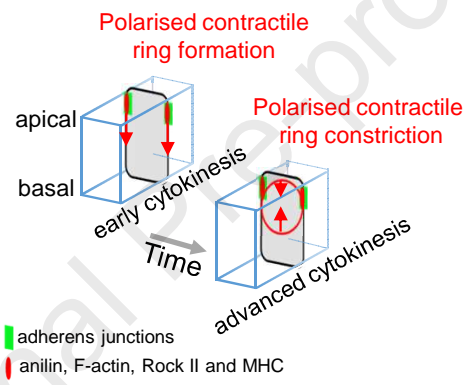
12

13

Author contributions

G.H. carried out the experiments, generated and interpreted the data. J-P.T. designed research and supervised the project. G.H., C.P. and J-P. T. wrote the manuscript.

Journal Pre-proof



1 Abstract

2

3 Cells dividing in the plane of epithelial tissues proceed by polarized constriction of the
4 actomyosin contractile ring, leading to asymmetric ingression of the plasma mem
5 brane. Asymmetric cytokinesis results in the apical positioning of the actomyosin
6 contractile ring and ultimately of the midbody. Studies have indicated that the
7 contractile ring is associated with adherens junctions, whose role is to maintain
8 epithelial tissue cohesion. However, it is yet unknown when the contractile ring
9 becomes associated with adherens junctions in epithelial cells. Here, we examined
10 contractile ring formation and activation in the epithelium of *Xenopus* embryos and
11 explored the implication of adherens junctions in the contractile ring formation. We
12 show that accumulation of proteins involved in contractile ring formation and
13 activation is polarized, starting at apical cell-cell contacts at the presumptive division
14 site and spreading within seconds towards the cell basal side. We also show that
15 adherens junctions are involved in the kinetics of contractile ring formation. Our study
16 reveals that the link between the adherens junctions and the contractile ring is
17 established from the onset of cytokinesis.

18

19

20

21

22 Keywords: cytokinesis, actomyosin, asymmetric furrowing, cell division, polarity

23

1 **1. Introduction**

2 Mitotic cells divide to produce two daughter cells in a process called cytokinesis,
3 which relies upon contraction of an actomyosin ring placed at the cell equator. The
4 contractile ring is constituted of actin filaments and the non-muscular motor protein
5 myosin II [1]. In isolated cells, the actomyosin ring contracts symmetrically, ingressing
6 the cell plasma membrane all around the mother cell midzone in an isoconcentric
7 manner. The contractile actomyosin ring must be accurately positioned at the
8 equatorial cortex to bisect the mitotic spindle and equally distribute the
9 chromosomes. This appropriate positioning is ensured by signals emanating from the
10 mitotic spindle in late anaphase. The building and contraction of the contractile
11 actomyosin ring requires activation of the small regulatory GTPase RhoA by the
12 GTPase Exchange Factor (GEF) Ect2. Centralspindlin, a heterotetramer of the
13 kinesin-related protein MLKP1 and the GTPase-activating protein (GAP)
14 MgcRacGAP, which interacts with microtubules of the central spindle, delivers Ect2
15 to the cell cortex, where it activates RhoA. Activated RhoA regulates simultaneously
16 the polymerization of actin filaments (F-actin) and activation of non-muscular myosin
17 II, thereby leading to constriction of the cytokinetic ring [1]. These regulations by
18 RhoA happen *via* concomitant activation of formins which increases actin
19 polymerisation and activation of the Rho-associated coiled-coil containing protein
20 kinase II (Rock II). Rock II in turn phosphorylates myosin light chain, thus activating
21 myosin. In addition to actin and myosin II, other proteins are components of the
22 contractile ring, including the scaffolding protein anillin which anchors the contractile
23 ring to the cell plasma membrane, maintains the furrow stability and is necessary for
24 effective RhoA-mediated contractility [2–5].

25 In contrast to the isoconcentric furrowing that occurs when isolated cells divide,
26 contraction of the actomyosin ring is polarized in cells dividing in the plane of an
27 epithelium, likely reflecting their marked apical-basolateral polarity. Furrowing
28 typically progresses from the cell's basal side towards the apical surface. This mode
29 of cytokinesis by asymmetric furrowing has been reported in diverse model systems,
30 including insects and vertebrates, suggesting that asymmetric furrowing is the default
31 mode of cytokinesis in epithelia [6,7]. Asymmetric furrowing is intimately linked to
32 epithelial cell polarity. Epithelial cells have distinct apical and basolateral plasma
33 membrane domains, separated by a belt of tight and adherens junctions [8–11].

1 Adherens junctions participate in the maintenance of epithelial tissue integrity. They
2 are constituted of the transmembrane protein cadherin, which creates, *via* its
3 extracellular domain, homophilic interactions with cadherin of neighbouring cells.
4 Through interactions of its intracytoplasmic tail with α and β -catenins, cadherin is
5 indirectly connected to the apical actomyosin belt, which maintains epithelial cell
6 shape and epithelial integrity.

7 In *Drosophila*, it has been shown that adherens junctions contribute to the asymmetry
8 of furrowing of dividing cells [12,13]. The cytokinetic ring constriction, which is
9 normally asymmetric in *Drosophila* epithelial cells, becomes symmetric in cells
10 depleted of β -catenin or E-cadherin. These studies demonstrate the importance of
11 adherens junctions for asymmetric furrowing and anchoring of the contractile ring for
12 apical positioning of the midbody. However, it remains largely unknown how the
13 contractile ring forms and when it becomes connected to adherens junctions.

14 Here, we used the epithelium of *Xenopus laevis* embryos at the gastrula stage to
15 study contractile ring formation, because at this developmental stage, cells divide
16 exclusively parallel to the epithelium plane such that both daughter cells remain
17 continuously in that plane [14]. Moreover, we have previously shown that epithelial
18 cells divide by asymmetric furrowing from the basal towards the apical side [15].
19 Using live imaging of *Xenopus laevis* gastrula embryos expressing several contractile
20 actomyosin ring components, we have here characterized the dynamics of contractile
21 ring formation and have shown that the contractile ring formation is polarized from
22 apical cell-cell junctions towards the cell basal side. Activation of the contractile motor
23 protein myosin II leading to the contraction of the actomyosin ring is also polarized.
24 Finally, we show that adherens junctions are involved in the formation kinetics of the
25 contractile ring.

26

27 **2. Materials and Methods**

28

29 *2.1 Plasmids*

30 Plasmids pCS2-Lifeact-GFP (a kind gift from Ulrike Engel, Heidelberg University,
31 Germany), pCS2-mRFP-GPI, pCS2-GFP-GPI (a kind gift from Mikael Brand,

1 Dresden University of Technology, Germany), pCS2-GFP-rGBD (a kind gift from
2 William Bement), pSp64T-C-cad Ctail [16], pT7T-ZO-1-GFP [17] and pT7T-SF9-GFP
3 [18] were used in this study. pT7T-GFP-Rock II K/R was constructed by site-directed
4 mutagenesis of lysine 117 (K117) from *Xenopus* Rock II (a kind gift from Johné Liu,
5 [19]). The K117, essential for the catalytic activity of the kinase, was replaced by an
6 arginine to abolish Rock II activity because the overexpression of the active kinase
7 causes division defects, which are not obtained with the Rock II K/R mutant. The
8 amplification product was cloned into the vector pT7T in phase with N-terminal GFP.
9 PT7T-3xGFP-anillin was constructed by PCR amplification of the *Xenopus* anillin
10 sequence, from the plasmid pT7T-GFP-Xlanillin [15] and subcloned into pT7T-3xGFP
11 with N-terminal 3xGFP. All new constructs were verified by sequencing. All plasmids
12 were linearised to generate mRNAs by *in vitro* transcription using the T7 or SP6
13 mMessage mMachine kit (Ambion).

14

15 2.2 α -catenin and ZO-1 knockdown

16 For α -catenin and ZO-1 knockdown experiments, antisense morpholinos targeting
17 the initiation codon of respectively α -catenin (5'-
18 ATGTTTCCTGTATTGAGAGTCATGC-3') and ZO-1 (5'-
19 GCCGGTGTCAGTATGAGTCCCCAGA-3') were produced by Gene Tools. These
20 morpholinos were previously characterized [17,20]. A standard morpholino (5'-
21 CTCTTACCTCAGTTACAATTTATA-3', Gene Tools) was used as a control.

22

23 2.3 Preparation of *Xenopus laevis* embryos and microinjection

24 *Xenopus laevis* albinos were obtained from Biological Resources Centre (CRB,
25 Rennes, France). All animal experiments were performed in accordance with the
26 approved protocols and guidelines at Rennes 1 University by the Comité Rennais
27 d'Ethique en Matière d'Expérimentation Animale (C2EA-07) and the French Ministry
28 for Education and Research (3523813). Eggs were fertilized *in vitro* and embryos
29 were collected as described previously [18]. After de-jelling, embryos were placed in
30 5% Ficoll in F1 buffer (10 mM HEPES pH 7.6, 31.2 mM NaCl, 1.75 mM KCl, 59 μ M
31 MgCl₂, 2 mM NaHCO₃, and 0.25 mM CaCl₂) for microinjection. mRNAs were

1 microinjected into one blastomere of 4- or 8-cell-stage embryos. For α -catenin
2 knockdown experiments, 20 ng of α -catenin antisense morpholino in 9.2 nl was
3 microinjected into one blastomere at the 8-cell stage. For α -catenin and ZO-1 double
4 knockdown, respectively 20 ng and 40 ng of morpholinos were microinjected.
5 Embryos were then placed at 16°C overnight and analyzed at the gastrula stage
6 (stage 11; [21]).

8 *2.4 Indirect immunofluorescence*

9 The embryos were fixed and treated as previously described (Hatte *et al.*, 2014).
10 Briefly, embryos were fixed with 2% trichloroacetic acid in 1× F1 buffer. After
11 embryos were devitellinated, cells were permeabilised in PBS+1% Triton X-100 for
12 20 min at room temperature, incubated in PBS+0.1% Triton X-100 (PBST 0.1%) for
13 10 min and then blocked for 1 h in 2% BSA in PBST 0.1% (BSA-PBST). Embryos
14 were incubated overnight in BSA-PBST at 14°C with a primary antibody.

15
16 The primary antibodies used in this study are directed against C-cadherin (DHSB,
17 6B6, 1:200), α -catenin (ThermoFisher Scientific, PA1-25081, 1:100), β -catenin
18 (Santa-Cruz, SC-7199, 1:100), F-actin (AC-40, Sigma, 1:200), phospho S20 myosin
19 regulatory light chain (MRLC, pS19 in *Xenopus laevis*, abcam, ab2480, 1:100),
20 MKLP1 (Santa Cruz, SC-867, 1:100), Ect2 (Millipore 1:100), *Xenopus laevis* anillin
21 and myosin heavy chain A (MHCA) (a kind gift from Aaron Straight, [4], 1:100),
22 *Xenopus laevis* Rock II (a kind gift from Johné Liu, [19] 1:100), ZO-1 (Zymed, 33-
23 9100, 1:200), occludin (a kind gift from Sandra Citi [22], 1:100), GFP (Roche, clone
24 7.1 and 13.1, 11914460001, 1:100) and mcherry (abcam, ab167453, 1:200).

25
26 After washing with PBST 0.1%, embryos were incubated with Alexa Fluor-488 or-555
27 anti-mouse, anti-rabbit or anti-sheep (ThermoFisher Scientific) and TO-PRO-3 to
28 stain DNA (Invitrogen, 0.5 μ g/ml) in BSA-PBST for 1 h at room temperature. After 3
29 washes of 5 min in 0.1% PBST, embryos were mounted in Vectashield (Vector).

30

1 For F-actin staining, embryos were fixed in 3.7% formaldehyde in F1 buffer for 2
2 hours at room temperature, permeabilised and blocked as previously described. After
3 blocking, embryos were incubated with AlexaFluor 555-conjugated Phalloidin (Life
4 Technologies, 1 U/ml) and TO-PRO3 for 2 h, washed and mounted in Vectashield.

5

6 *2.5 Lambda phosphatase treatment of embryos*

7 Embryos fixed in TCA, as previously described, were incubated in the appropriate
8 buffer with or without 25 units of lambda phosphatase (New England Biolabs) at 30°C
9 for 30 min. Embryos were then extensively washed with PBS, permeabilized and
10 proceed for indirect immunofluorescence with the anti-phospho S20 myosin
11 regulatory light chain as the primary antibody.

12

13 *2.6 Confocal microscopy on living and fixed embryos*

14 For immunofluorescence, a Leica SP5 confocal microscope with an oil immersion
15 objective 40x / 1.25-0.75 HC PL APO (WD 0.1 mm) was used. Imaging of live
16 embryos was performed with a Leica SP8 confocal microscope with a 63x / 1.4 HC
17 PL APO oil objective, using a resonant scanner. This scanner allows extremely fast
18 acquisitions (scanning frequency of 8000 Hz), essential for analyzing the recruitment
19 of proteins into the contractile ring.

20

21 *2.7 Quantification of immunolabelling at adherens and tight junctions*

22 To test if contractile ring activation could be polarized along the apical-basal cell axis,
23 the fluorescence intensities of Rock II and pS19MRLC detected by immunolabelling
24 in fixed embryos were quantified. Because Rock II localises at the apical junctional
25 complex and is distributed along the lateral membrane several μm below (Fig. 1B),
26 quantification of fluorescence intensity was standardized by measuring 10 μm below
27 the apical cell-cell junctions. At this distance, the fluorescence intensity was minimal.
28 In contrast, pS19MRLC fluorescence is more restricted to apical cell-cell contacts
29 compared to Rock II (Fig. 1B), therefore quantification was standardized by
30 measuring 5 μm below apical junctions. For both Rock II and pS19MRLC,

1 fluorescence intensities were also measured at non-furrowing faces, orthogonal to
2 the division site (hereafter referred as cell poles). To quantify fluorescence intensity
3 for Rock II and pS19MRLC, the mean pixel intensity was measured in a region of
4 interest (ROI) at the cell-cell contacts. This ROI was placed at the division site for
5 cells already engaged in cytokinesis or perpendicularly and equally distant from
6 mitotic chromosomes. The mean fluorescence pixel intensity in proximity to the
7 presumptive division site was measured in a ROI with identical size to the ROI used
8 for quantification at the division site and was subtracted from the pixel intensity at the
9 division site.

10

11 *2.9 Quantification of the duration of ring contraction and contractile ring formation*

12 The duration of the ring contraction was calculated by subtracting the time when the
13 contractile ring begins to contract at the basal side to the time when it is fully
14 ingressed and concentrates at the apical pole of the cell. For the duration of the
15 contractile ring formation, the time when the protein of interest begins to accumulate
16 at the presumptive division site was subtracted from the time when the contractile
17 ring begins to constrict at the basal side.

18

19 *2.10 Image processing and quantification*

20 Images were processed using ImageJ software (Rasband, W.S.,
21 <http://rsb.info.nih.gov/ij>) and figures were prepared using ImageJ and Photoshop.
22 Graphing was performed using Microsoft Excel. Kymographs of lateral cell-cell
23 contacts were mounted manually.

24

25 *2.11 Statistical analysis*

26 No statistical method was used to predetermine the sample size. The experiments
27 were not randomized and investigators were not blinded to allocation during
28 experiments and outcome assessment. Experiments were repeated at least two
29 times. Sample sizes are indicated for each experiment in figure legends. A two-tailed
30 unpaired Student t-test was applied to determine statistical significance. Statistical
31 analysis was performed using Microsoft Excel software except for Rock II and

1 pS19MRLC fluorescence pixel intensities at the division sites and poles for which a
2 Mann Whitney test was done using Prism software.

3

4

5

6 **3. Results**

7

8 *3.1 The proteins involved in cytokinesis localize at the apical junctional complex in* 9 *the Xenopus laevis embryo*

10 First and foremost, we studied the formation of the actomyosin contractile ring by
11 examining the localization of several proteins involved in cytokinesis in the epithelium
12 of *Xenopus laevis* embryo. In non-dividing cells, filamentous actin (F-actin) and
13 myosin heavy chain A (MHCA) localize at apical cell-cell contacts where they form a
14 contractile belt at the apical cell periphery (Fig. 1A). On orthogonal projections,
15 proteins appear as dots extended by faint signals which intensity decreases along
16 the lateral cell-cell contacts (Fig. 1A, arrowheads on orthogonal views). The F-actin
17 signal decreases along the lateral cell cortex whereas β -catenin was localized all
18 around the basolateral cell contacts (Fig. 1B; [23]) indicating that the decrease of F-
19 actin signal is specific. MHCA was also detected in the cytoplasm and at the medial
20 cortex. Anillin, a scaffolding protein which interacts with F-actin and myosin, also
21 localise at the apical cell-cell contacts and into nuclei (Fig. 1A), as described
22 previously [3]. As previously shown in cultured cells [24], the two regulators of
23 cytokinesis, MKLP1, a constituent of the centralspindlin complex and Ect2, an
24 activator of Rho GTPase, localize at apical cell-cell contacts (Fig. S1A and S1C). We
25 also examined the localisation of the protein kinase Rock II which activates myosin
26 by phosphorylating the serine 20 residue (serine 19 in *Xenopus laevis*) of the myosin
27 regulatory light chain (MRLC) leading to the contraction of the actomyosin contractile
28 ring during cytokinesis [25]. The activated MRLC was detected with an antibody
29 recognizing the MRLC serine 19 phosphorylation (pS19MRLC). Both proteins, Rock
30 II and activated myosin, co-localize with C-cadherin at the adherens junctions,
31 although pS19MRLC was more restricted towards apical side unlike Rock II (Fig. 1C).

1 Our results show that all the key proteins involved in cytokinesis that we examined
2 localize to the apical cell-cell contacts in the *Xenopus* embryo epithelium.

3

4 *3.2 Accumulation of contractile ring components begins at apical cell-cell contacts* 5 *and expands basally along the lateral membrane*

6 To study the formation dynamics of the actomyosin contractile ring in epithelial cells,
7 we expressed four distinct fluorescent proteins in embryos. We expressed the two
8 proteins involved in cytokinesis, Rock II K/R, a catalytically inactive form of Rock II
9 and anillin tagged with GFP (respectively GFP-Rock II K/R and 3xGFP-anillin) and
10 used two fluorescent probes: the SF9-GFP intrabody, which detects the endogenous
11 myosin heavy chain A (MHCA) [26], and GFP-Lifeact which detects F-actin [27]. As
12 described above for endogenous proteins, all the four proteins localized at the apical
13 cell-cell junctions (Fig. 2 A-D and Fig. S2A). Expression of these fluorescent proteins
14 has no significant impact on the duration of ring contraction compared with cells
15 expressing GFP fused with a glycosylphosphatidylinositol (GPI)-anchor (GFP-GPI)
16 used to visualize cells plasma membrane (Fig. S2B, mean duration of ring
17 contraction 5 min 50 s). During cytokinesis, the four proteins that we tested localize at
18 the contractile ring (Fig. 2A-D, white arrowheads on front views, see Fig. S2C for an
19 example of full cytokinesis and asymmetric constriction of the contractile ring in a cell
20 expressing 3xGFP-anillin). Interestingly, very shortly before plasma membrane
21 ingression starts at the basal side, the fluorescence intensity of the four proteins
22 increases at the apical cell-cell contacts at the presumptive plasma membrane
23 ingression site (Fig. 2 A-D, dashed circles on front views, orthogonal views). The
24 extent to which fluorescence intensities increased depended on the fluorescent
25 protein, with 3xGFP-anillin increasing more than the 3 others (Fig. 2 A-D,
26 histograms). Subsequently, fluorescence spreads and fluorescence intensity
27 increases with time along the baso-lateral membrane (Fig. 2 A-D, kymographs and
28 histograms). The time elapsed between the beginning of accumulation of the four
29 proteins at the apical cell-cell contacts and the beginning of plasma membrane
30 ingression at the basal side ranges from 12 s. to 55 s. (Fig 2E, mean time: 30
31 seconds). Such a dynamic localization does not occur for GFP-GPI nor for the tight
32 junction protein ZO-1, which follows the plasma membrane shape modifications
33 without additional accumulation compared to non-dividing cells (Fig. S3A and S3B).

1 In epithelial cells of the *Xenopus* embryos, the mitotic spindle position along the
2 apicobasal axis is stereotypically biased toward the apical surface (Fig. S4 and [23]).
3 Because in late anaphase, the mitotic spindle signals to the cell cortex the position of
4 the contractile ring, the asymmetrically positioned mitotic spindle could be involved in
5 the apical-to-basal accumulation of contractile ring proteins. Interestingly, the two
6 cytokinesis regulators, MKLP1 and Ect2, localized at apical and lateral cell-cell
7 contacts in anaphase cells (Fig. S1B and S1D, respectively). This result suggests
8 that the asymmetrically positioned mitotic spindle could drive the apical recruitment of
9 the contractile ring proteins.

10 In summary, the four proteins involved in cytokinesis, which we examined, start to
11 accumulate at the presumptive division site asymmetrically from the apical cell-cell
12 contacts and expand along the lateral cell plasma membrane towards the basal side.

13

14 *3.3 Activation of the actomyosin contractile ring is polarized*

15 The finding that contractile ring components accumulate asymmetrically led to the
16 question of whether activation of the actomyosin contractile ring could be polarized
17 along the apical-basal cell axis. Since RhoA is a master regulator of actomyosin ring
18 activation, we thought to use the GFP-rGBD probe [28] to follow active RhoA in living
19 embryos. Fluorescence of the GFP-rGBD probe was detected at cell-cell contacts in
20 non-dividing cells and at the contractile ring in cells advanced in cytokinesis (Fig.
21 S5A). However, the fluorescence in the cytoplasm was also high (cells expressing
22 high and low levels of GFP-rGBD are shown in Fig. S5A) which turned out to be
23 incompatible with the high temporal resolution needed to image GFP-rGBD at the
24 presumptive division site. This issue made the GFP-rGBD probe unusable for our
25 study on the early steps of cytokinesis. To overcome this challenge, we investigated
26 the localization of the myosin II regulatory light chain phosphorylated on serine 19
27 (pS19MRLC) in fixed embryos. S19 phosphorylation, which is catalysed by Rock II,
28 induces myosin activation and subsequently actomyosin constriction. To validate the
29 approach based on fixed material, we first studied Rock II localization, as we have
30 previously shown the polarized accumulation of GFP-Rock II KR at the presumptive
31 division site. Immunofluorescence signal of Rock II was indistinguishable between
32 cells in metaphase and at the very beginning of anaphase, when chromosomes start

1 splitting (these cells will be referred as early anaphase, Fig. 3A). However, in cells
2 more advanced in anaphase, Rock II signal was detected deeper along the lateral
3 plasma membrane. Hereafter, these cells advanced in anaphase, showing Rock II
4 accumulation but without any sign of plasma membrane ingression will be referred as
5 early cytokinesis (Fig. 3A, compare orthogonal views at the division site of early
6 anaphase with early cytokinesis). In cells more advanced in cytokinesis, the
7 ingressed plasma membrane was generally fully labelled by the anti-Rock II antibody
8 (Fig. 3A). However, for some unknown reason, we also frequently observed
9 incomplete labelling at the base of the contractile ring. A similar observation of
10 incomplete ring labelling was previously reported in living tissues of *Drosophila* [29].
11 Rock II fluorescence intensity was quantified at the presumptive division site in early
12 anaphase and early cytokinesis cells. For comparison, in the same cells, we also
13 quantified Rock II signal at the cell poles (non-furrowing faces orthogonal to the
14 division site). The quantitative analysis shows a significant statistical difference
15 between Rock II intensity at the presumptive division site compared to cell poles (Fig.
16 3B). Moreover, at the presumptive division site, Rock II signal intensity increases with
17 the length of plasma membrane labelled for Rock II (Fig. 3C). Although Rock II signal
18 intensity also increases at the cell poles, this increase was less marked compared to
19 the presumptive division site (Fig. 3C, equation of linear regressions are given for
20 poles and division site). The correlation between Rock II accumulation and the length
21 of the plasma membrane labelled for Rock II suggests that the Rock II signal
22 expands along the baso-lateral membrane. This result is in agreement with the
23 previously shown polarized accumulation of the GFP-Rock II K/R probe in living
24 embryos. Therefore, we used indirect immunofluorescence with fixed embryos to
25 study myosin activation.

26 Fixed embryos were labelled with an anti-pS19 MRLC antibody, the specificity of
27 which was previously validated (Fig. S5B). As previously observed for Rock II,
28 pS19MRLC signal was indistinguishable between cells in metaphase and early
29 anaphase (Fig. 3D). As previously quantified for Rock II, fluorescence intensities
30 were also quantified at the division site and at the cell poles. Quantifications show a
31 significant statistical difference between pS19MRLC fluorescence intensity at the
32 presumptive division site compared to cell poles (Fig. 3E). Moreover, pS19MRLC
33 signal intensity increases with the length of the plasma membrane labelled for

1 pS19MRLC at the presumptive cell division site whereas it remained almost
2 unchanged at the cell poles (Fig. 3F). These results are consistent with the
3 phosphorylation of the myosin regulatory light chain being polarized, starting at the
4 apical cell-cell junctions and spreading along the lateral membrane towards the basal
5 side.

6 Altogether, our results show that accumulation of proteins constituting the actomyosin
7 contractile ring, and activation of the ring start at the apical cell-cell contacts and
8 expands along the lateral membrane. Since furrowing progresses in the basal to
9 apical orientation, the reverse polarity of the contractile ring formation was
10 unexpected.

11

12 *3.4 The adherens junctions are involved in the polarized formation of the contractile* 13 *ring*

14 Our results show that cytokinetic proteins co-localise with adherens junctions and the
15 assembly and activation of the cytokinetic contractile ring begins at the apical cell-cell
16 contacts. Due to the close link previously shown between cytokinesis and the
17 adherens junctions [12,13,28,29, 35], we examined if adherens junctions could be
18 involved in the asymmetric formation of the contractile ring.

19 To interfere with the adherens junctions, we followed two distinct approaches. In the
20 first approach, we used a deletion mutant corresponding to the cytosolic domain of C-
21 cadherin (Ctail) [16]. C-cadherin (also termed EP-cadherin) is the main adherens
22 junctions molecule of the *Xenopus* gastrula [31,32]. Because the extra-cellular and
23 the trans-membrane domains are missing in the Ctail, it is unable to integrate the
24 plasma membrane and bridge with C-cadherin of neighbouring cells. However, the
25 cytosolic domain of E-cadherin is responsible for indirect binding with the F-actin *via*
26 interaction with α and β catenins. It has been shown that the ubiquitous expression in
27 the *Xenopus* embryos of high levels of Ctail provokes cell dissociation [16]. This loss
28 of cell-cell contacts indicated a decrease in cell adhesion suggesting that the Ctail
29 could act as a dominant-negative mutant by titrating catenins. Because the mode of
30 action of Ctail was not described in details, we further characterized this mutant. The
31 Ctail mutant was co-expressed together with GFP or RFP -GPI used as tracers, and
32 we examined the expression of diverse proteins localized at the adherens junctions.

1 Unlike control cells, the apical membrane of cells expressing Ctail was frequently
2 round (Fig. 4A, compare orthogonal views of control and Ctail), suggesting a
3 decrease in cell-cell adhesion as previously reported by Lee and Gumbiner [16]. The
4 amounts of endogenous C-cadherin, α and β -catenins, F-actin and Rock II, localized
5 at the adherens junctions, were significantly decreased in cells expressing Ctail (Fig.
6 4A, histograms). In contrast, localization of two constituents of the tight junctions, ZO-
7 1 and occludin, was not affected (Fig. S6). Our results show that expression of Ctail
8 disrupts the adherens junctions, which could explain epithelial structural defects
9 observed in our and previous studies [16].

10 We then tested if the expression of the Ctail mutant could affect the formation and
11 contraction of the actomyosin ring. In both control and Ctail expressing cells, Lifeact-
12 GFP and 3xGFP-anillin fluorescence appears apically and expands along the lateral
13 membrane (Fig. 4B and 4D, upper rows). The asymmetric contraction of the
14 actomyosin ring from the basal side towards the apical side was also unaffected by
15 Ctail expression (Fig. 4B and 4D, lower rows).

16 Interestingly, the time elapsed between the beginning of the accumulation of Lifeact-
17 GFP and 3xGFP-Anillin at the apical cell-cell contacts and the beginning of plasma
18 membrane ingression at the basal side significantly increased in Ctail expressing
19 cells compared to controls (58.9 \pm 7.2 s vs 30.7 \pm 10.4 s for Lifeact-GFP and 54.2 \pm -
20 13.1 s vs 21.4 \pm 5.9 s for 3xGFP-Anillin, respectively Fig. 4C and 4E). This result
21 suggested that the adherens junctions could be involved in the polarized recruitment
22 of the contractile ring components. To test this hypothesis, we followed a second
23 approach to interfere with the adherens junctions.

24 In the second approach, we used an antisense morpholino oligonucleotide to deplete
25 α -catenin, which indirectly links C-cadherin to the actomyosin cytoskeleton (Mo α -cat,
26 Fig. 5A). As previously shown [20,33], depletion of α -catenin also led to a significant
27 decrease of C-cadherin (Fig. 5A) and perijunctional actin filaments (not shown, [17]).
28 This result shows that Mo α -cat, by depleting α -cat, destabilizes the adherens
29 junctions. Measurement of the time lasting from the beginning of fluorescence
30 increase and the start of ring constriction shows that the recruitment durations of
31 Lifeact-GFP and 3xGFP-anillin at the apical cell-cell contacts significantly increases
32 in Mo α -cat treated cells compared with control morpholino (MoCo) cells (57.3 \pm 13.0
33 s vs 33.1 \pm 11.0 s for Lifeact-GFP and 41.5 \pm 8.0 s vs 27.6 \pm 4.0 s, respectively Fig.

1 5B and 5C, histograms). As with the Ctail mutant, the polarized recruitment of Lifeact-
2 GFP and 3xGFP-anillin occurred in cells treated with MoCo as well as cells treated
3 with Mo α -cat (Fig. 5B and 5C). The subsequent asymmetric ring constriction also
4 normally occurred (not shown and [17] for Lifeact-GFP). To test if tight junctions may
5 contribute in maintaining the asymmetric ring constriction in α -cat depleted cells,
6 embryos were microinjected with Mo α -cat, Mo ZO-1 and 3xGFP-anillin mRNA. ZO-1
7 is a tight junction-associated protein. As previously shown with ZO-1 disruption alone
8 [17], disruption of tight and adherens junctions led to prolonged cytokinesis and
9 flattened contractile ring with normal asymmetry (Fig. S7).

10 Altogether, these results indicate that the adherens junctions are involved in the
11 polarized accumulation of the contractile ring components at the presumptive division
12 site.

13

14

15 **4. Discussion**

16

17 In the present study, we have shown that at cytokinesis onset the levels of proteins
18 forming and activating the contractile actomyosin ring increase at the apical cell-cell
19 contacts. The initiation of ring formation at the apical contacts could appear in
20 contradiction with the asymmetric furrowing which progresses from the basal side
21 towards the apical side. However, our results show that the ring formation is
22 extremely rapid, occurring in approximately 30 seconds before the first sign of ring
23 constriction. Moreover, we have shown that ring formation spread laterally from
24 apical contacts towards the basal side of cells.

25 Cytokinesis by asymmetric furrow ingression is closely linked to the presence of an
26 apical junctional complex in epithelial cells. Indeed, the actomyosin contractile ring
27 remains associated with apically localized adherens junctions in *Drosophila* [12,13].
28 In vertebrates, the apical junctional complex continuously contacts the contractile ring
29 [34–36]. Moreover, in *Drosophila*, it has been shown that interfering with the
30 adherens junctions causes the furrow to become symmetric [12,13]. Although these
31 observations showed that the contractile ring is associated with the adherens
32 junctions, they did not elucidate when the two structures become associated. In the

1 present study, we show that the adherens junctions are involved in the polarized
2 contractile ring formation.

3 Although interfering with adherens junctions increased the duration of accumulation
4 of proteins forming the contractile ring, it did not abolish the asymmetric contraction
5 of the ring. These results are in contrast with previous studies in *Drosophila* in which
6 it was shown that knockdown by RNAi of E-cadherin and α -catenin or in armadillo
7 (the *Drosophila* orthologue of β -catenin) mutant, constriction of the actomyosin ring
8 becomes symmetric [12,13]. The remaining amounts of junctional proteins at the
9 adherens junctions observed in Ctail expressing cells and α -catenin knocked down
10 cells could be sufficient to maintain asymmetric constriction of the contractile ring as
11 noticed in our study. However, in Ctail cells, we frequently observed a rounding of
12 cell indicative of a decrease in cell adhesion, which should have affected the
13 asymmetric furrowing. The discrepancy between our results and results obtained in
14 *Drosophila* regarding the asymmetric ring constriction may originate from the distinct
15 models used. The organization of adherens and tight (septate in *Drosophila*)
16 junctions differ in vertebrates and insects. Moreover, cytokinesis also exhibit marked
17 difference in the two models including the maintenance of contacts of apical junctions
18 with the contractile ring [35]. It is possible that the tight junctions, by maintaining
19 mechanical strain on the cell plasma membrane, could be involved in the
20 maintenance of asymmetric constriction of the contractile ring. In this respect, we
21 observed that tight junctions were unaffected by expression of the Ctail mutant. The
22 double disruption of tight and adherens junctions led to flattened contractile ring and
23 altered cytokinesis duration (Fig. S7), as previously shown for tight junction disruption
24 alone which increases mechanical tension applied on adherens junctions [17]. In the
25 double knockdown, it is possible that ZO-1 depletion could lead, *via* remaining
26 adherens junction proteins, to an increase of mechanical tension applied on
27 adherens junctions and normal ring contraction asymmetry. As the mechanism
28 leading to the increase of mechanical tension applied to adherens junctions upon
29 ZO-1 depletion is unknown, the hypothesis of tight junctions involvement in
30 asymmetric contraction of the contractile ring will require further investigations.

31 In epithelial cells of *Xenopus* embryos, the mitotic spindle position is stereotypically
32 biased toward the apical cell side [23] and (Fig. S4). This result suggests that the
33 asymmetric apicobasal position of the mitotic spindle could be involved in

1 accumulation of contractile ring proteins starting at apical cell-cell contacts of the
2 presumptive division site. Our results suggest that in dividing epithelial cells, the
3 signalling pathway leading to the contractile ring activation could be focused on
4 adherens junctions (Fig. 5D). As microtubules are known to be involved in the
5 signalling which induces cytokinesis [1], it will be of interest to explore their putative
6 implication in the polarized accumulation of contractile ring proteins.

7 Interestingly, all proteins involved in cytokinesis analysed in the present study
8 localize at the apical cell-cell contacts before cytokinesis onset. The previous studies
9 showing that the centralspindlin complex, Ect2 and anillin regulate the Rho GTPase
10 cycle at the adherens junctions indicated that they could participate in apical
11 junctions' homeostasis [3,24,37]. Conversely, it has been shown that depletion of α -
12 catenin in MCF-7 epithelial cells reduces Ect2 levels at the adherens junctions [24],
13 indicating that the adherens junctions are involved in recruiting components involved
14 in the actomyosin contractility of the perijunctional belt in non-dividing cells.

15 Consequently, our results showing that adherens junctions are involved in the ring
16 formation extend their implication to the contractile ring components during
17 cytokinesis. Additional studies will be required to understand in details the highly
18 dynamic mechanisms supporting the recruitment of cytokinetic proteins at the onset
19 of epithelial cell cytokinesis.

20 Studies of cytokinesis in epithelial tissues have revealed the basal to the apical
21 asymmetry of the contractile ring contraction. However, before contraction, the cell
22 plasma membrane and the underneath contractile ring need to be freed from
23 extracellular contacts at their basal side [38–40]. Our study raises the question of
24 how epithelial cells precisely orchestrate polarized contractile ring formation and
25 activation with basal membrane disengagement.

26

27

28 **5. Conclusions**

29 Our study highlight the involvement of adherens junctions in the polarized formation
30 and activation of the actomyosin contractile ring at the onset of cytokinesis. Our
31 results give a simple explanation to the previously reported association of the
32 actomyosin contractile ring with apical junctional complex during cytokinesis.

1
2
3
4
5
6
7
8
9
10
11
12
13
14
15
16
17
18
19
20
21
22
23
24
25
26
27
28
29

Acknowledgements

We are grateful to Michael Danilchik, Arun Prasath Damodaran (C. Prigent's team) and Roland Le Borgne for critical reading on the manuscript. We thank the Microscopy Rennes Imaging Center (MRic, BIOSIT, IBiSA). This work was supported by the Centre National de la Recherche Scientifique (CNRS) and the Ligue Contre le Cancer (comités 29 et 35). G.H. was supported by the Ministère de l'Enseignement Supérieur, de la Recherche et de l'Innovation and partly by a grant from the Ligue Nationale Contre le Cancer.

Author contributions

G.H. carried out the experiments, generated and interpreted the data. J-P.T. designed research and supervised the project. G.H. C.P. and J-P. T. wrote the manuscript.

Conflict of interest

The authors declare no conflict of interest.

References

- [1] P.P. D'Avino, M.G. Giansanti, M. Petronczki, Cytokinesis in animal cells, Cold Spring Harb. Perspect. Biol. 7 (2015).
<https://doi.org/10.1101/cshperspect.a015834>.
- [2] A.J. Piekny, M. Glotzer, Anillin Is a Scaffold Protein That Links RhoA, Actin, and Myosin during Cytokinesis, Curr. Biol. (2008).
<https://doi.org/10.1016/j.cub.2007.11.068>.

- 1 [3] C.C. Reyes, M. Jin, E.B. Breznau, R. Espino, R. Delgado-Gonzalo, A.B.
2 Goryachev, A.L. Miller, Anillin regulates cell-cell junction integrity by organizing
3 junctional accumulation of Rho-GTP and actomyosin, *Curr. Biol.* (2014).
4 <https://doi.org/10.1016/j.cub.2014.04.021>.
- 5 [4] A.F. Straight, C.M. Field, T.J. Mitchison, Anillin binds nonmuscle myosin II and
6 regulates the contractile ring, *Mol. Biol. Cell.* 16 (2005).
7 <https://doi.org/10.1091/mbc.E04-08-0758>.
- 8 [5] J. Liu, G.D. Fairn, D.F. Ceccarelli, F. Sicheri, A. Wilde, Cleavage furrow
9 organization requires PIP 2-mediated recruitment of anillin, *Curr. Biol.* (2012).
10 <https://doi.org/10.1016/j.cub.2011.11.040>.
- 11 [6] S. Le Bras, R. Le Borgne, Epithelial cell division - Multiplying without losing
12 touch, *J. Cell Sci.* (2014). <https://doi.org/10.1242/jcs.151472>.
- 13 [7] J.P. Tassan, M. Wühr, G. Hatte, J. Kubiak, Asymmetries in cell division, cell
14 size, and furrowing in the *xenopus laevis* embryo, in: *Results Probl. Cell Differ.*,
15 2017. https://doi.org/10.1007/978-3-319-53150-2_11.
- 16 [8] M.C. Gibson, N. Perrimon, Apicobasal polarization: Epithelial form and
17 function, *Curr. Opin. Cell Biol.* (2003).
18 <https://doi.org/10.1016/j.ceb.2003.10.008>.
- 19 [9] E. Rodriguez-Boulan, I.G. Macara, Organization and execution of the epithelial
20 polarity programme, *Nat. Rev. Mol. Cell Biol.* (2014).
21 <https://doi.org/10.1038/nrm3775>.
- 22 [10] U. Tepass, The apical polarity protein network in *drosophila* epithelial cells:
23 Regulation of polarity, junctions, morphogenesis, cell growth, and survival,
24 *Annu. Rev. Cell Dev. Biol.* (2012). <https://doi.org/10.1146/annurev-cellbio-092910-154033>.
- 25
- 26 [11] B.J. Thompson, Cell polarity: Models and mechanisms from yeast, worms and
27 flies, *Dev.* (2013). <https://doi.org/10.1242/dev.083634>.
- 28 [12] E. Morais-De-Sá, C. Sunkel, Adherens junctions determine the apical position
29 of the midbody during follicular epithelial cell division, *EMBO Rep.* (2013).
30 <https://doi.org/10.1038/embor.2013.85>.

- 1 [13] C. Guillot, T. Lecuit, Adhesion Disengagement Uncouples Intrinsic and
2 Extrinsic Forces to Drive Cytokinesis in Epithelial Tissues, *Dev. Cell.* (2013).
3 <https://doi.org/10.1016/j.devcel.2013.01.010>.
- 4 [14] A.D. Chalmers, B. Strauss, N. Papalopulu, Oriented cell divisions
5 asymmetrically segregate aPKC and generate cell fate diversity in the early
6 *Xenopus* embryo, *Development.* (2003). <https://doi.org/10.1242/dev.00490>.
- 7 [15] Y. Le Page, I. Chartrain, C. Badouel, J.-P. Tassan, A functional analysis of
8 MELK in cell division reveals a transition in the mode of cytokinesis during
9 *Xenopus* development, *J. Cell Sci.* 124 (2011).
10 <https://doi.org/10.1242/jcs.069567>.
- 11 [16] C.H. Lee, B.M. Gumbiner, Disruption of gastrulation movements in *Xenopus* by
12 a dominant-negative mutant for C-cadherin, *Dev. Biol.* (1995).
13 <https://doi.org/10.1006/dbio.1995.1288>.
- 14 [17] G. Hatte, C. Prigent, J.-P. Tassan, Tight junctions negatively regulate
15 mechanical forces applied to adherens junctions in vertebrate epithelial tissue,
16 *J. Cell Sci.* 131 (2018). <https://doi.org/10.1242/jcs.208736>.
- 17 [18] G. Hatte, M. Tramier, C. Prigent, J.P. Tassan, Epithelial cell division in the
18 *Xenopus laevis* embryo during gastrulation, *Int. J. Dev. Biol.* (2014).
19 <https://doi.org/10.1387/ijdb.140277jt>.
- 20 [19] S. Farah, Y. Agazie, N. Ohan, J.K. Ngsee, X.J. Liu, A Rho-associated protein
21 kinase, ROK α , binds insulin receptor substrate-1 and modulates insulin
22 signaling, *J. Biol. Chem.* (1998). <https://doi.org/10.1074/jbc.273.8.4740>.
- 23 [20] S. Nandadasa, Q. Tao, A. Shoemaker, S. wook Cha, C. Wylie, Regulation of
24 classical cadherin membrane expression and F-actin assembly by alpha-
25 catenins, during *Xenopus* embryogenesis, *PLoS One.* (2012).
26 <https://doi.org/10.1371/journal.pone.0038756>.
- 27 [21] P.D. Nieuwkoop, J. Faber, Normal Table of *Xenopus laevis* (Daudin)., North-
28 Holl, Amsterdam, 1967.
- 29 [22] M. Corderionsi, E. Mazzon, L. De Rigo, S. Baraldo, F. Meggio, S. Citi, Occludin
30 dephosphorylation in early development of *Xenopus laevis*, *J. Cell Sci.* (1997).

- 1 [23] S. Woolner, N. Papalopulu, Spindle Position in Symmetric Cell Divisions during
2 Epiboly Is Controlled by Opposing and Dynamic Apicobasal Forces, *Dev. Cell.*
3 (2012). <https://doi.org/10.1016/j.devcel.2012.01.002>.
- 4 [24] A. Ratheesh, G.A. Gomez, R. Priya, S. Verma, E.M. Kovacs, K. Jiang, N.H.
5 Brown, A. Akhmanova, S.J. Stehbens, A.S. Yap, Centralspindlin and α -catenin
6 regulate Rho signalling at the epithelial zonula adherens, *Nat. Cell Biol.* (2012).
7 <https://doi.org/10.1038/ncb2532>.
- 8 [25] M. Amano, M. Ito, K. Kimura, Y. Fukata, K. Chihara, T. Nakano, Y. Matsuura,
9 K. Kaibuchi, Phosphorylation and activation of myosin by Rho-associated
10 kinase (Rho-kinase), *J. Biol. Chem.* (1996).
11 <https://doi.org/10.1074/jbc.271.34.20246>.
- 12 [26] C. Nizak, S. Martin-Lluesma, S. Moutel, A. Roux, T.E. Kreis, B. Goud, F. Perez,
13 Recombinant antibodies against subcellular fractions used to track endogenous
14 Golgi protein dynamics in vivo, *Traffic.* (2003). [https://doi.org/10.1034/j.1600-](https://doi.org/10.1034/j.1600-0854.2003.00132.x)
15 [0854.2003.00132.x](https://doi.org/10.1034/j.1600-0854.2003.00132.x).
- 16 [27] J. Riedl, A.H. Crevenna, K. Kessenbrock, J.H. Yu, D. Neukirchen, M. Bista, F.
17 Bradke, D. Jenne, T.A. Holak, Z. Werb, M. Sixt, R. Wedlich-Soldner, Lifeact: A
18 versatile marker to visualize F-actin, *Nat. Methods.* (2008).
19 <https://doi.org/10.1038/nmeth.1220>.
- 20 [28] H.A. Benink, W.M. Bement, Concentric zones of active RhoA and Cdc42
21 around single cell wounds, *J. Cell Biol.* (2005).
22 <https://doi.org/10.1083/jcb.200411109>.
- 23 [29] N. Founounou, N. Loyer, R. Le Borgne, Septins Regulate the Contractility of
24 the Actomyosin Ring to Enable Adherens Junction Remodeling during
25 Cytokinesis of Epithelial Cells, *Dev. Cell.* 24 (2013) 242–255.
26 <https://doi.org/10.1016/j.devcel.2013.01.008>.
- 27 [30] S. Herszterg, A. Leibfried, F. Bosveld, C. Martin, Y. Bellaiche, Interplay
28 between the Dividing Cell and Its Neighbors Regulates Adherens Junction
29 Formation during Cytokinesis in Epithelial Tissue, *Dev. Cell.* 24 (2013) 256–
30 270. <https://doi.org/10.1016/j.devcel.2012.11.019>.
- 31 [31] Y.S. Choi, R. Sehgal, P. McCrea, B. Gumbiner, A cadherin-like protein in eggs

- 1 and cleaving embryos of *Xenopus laevis* is expressed in oocytes in response to
2 progesterone, *J. Cell Biol.* (1990). <https://doi.org/10.1083/jcb.110.5.1575>.
- 3 [32] D. Ginsberg, D. DeSimone, B. Geiger, Expression of a novel cadherin (EP-
4 cadherin) in unfertilized eggs and early *Xenopus* embryos, *Development*.
5 (1991).
- 6 [33] G. Hatte, C. Prigent, J.P. Tassan, Tight junctions negatively regulate
7 mechanical forces applied to adherens junctions in vertebrate epithelial tissue,
8 *J. Cell Sci.* (2018). <https://doi.org/10.1242/jcs.208736>.
- 9 [34] J. Baker, D. Garrod, Epithelial cells retain junctions during mitosis., *J. Cell Sci.*
10 104 (Pt 2 (1993) 415–425.
- 11 [35] T. Higashi, T.R. Arnold, R.E. Stephenson, K.M. Dinshaw, A.L. Miller,
12 Maintenance of the Epithelial Barrier and Remodeling of Cell-Cell Junctions
13 during Cytokinesis, *Curr. Biol.* 26 (2016) 1829–1842.
14 <https://doi.org/10.1016/j.cub.2016.05.036>.
- 15 [36] Y. Jinguji, H. Ishikawa, Electron microscopic observations on the maintenance
16 of the tight junction during cell division in the epithelium of the mouse small
17 intestine., *Cell Struct. Funct.* 17 (1992) 27–37.
18 <http://www.ncbi.nlm.nih.gov/pubmed/1586965>.
- 19 [37] A. Rosa, E. Vlassaks, F. Pichaud, B. Baum, Ect2/Pbl Acts via Rho and Polarity
20 Proteins to Direct the Assembly of an Isotropic Actomyosin Cortex upon Mitotic
21 Entry, *Dev. Cell.* (2015). <https://doi.org/10.1016/j.devcel.2015.01.012>.
- 22 [38] K.G. Bourdages, B. Lacroix, J.F. Dorn, C.P. Descovich, A.S. Maddox,
23 Quantitative analysis of cytokinesis In Situ during *C. Elegans* postembryonic
24 development, *PLoS One.* (2014). <https://doi.org/10.1371/journal.pone.0110689>.
- 25 [39] D.J. Fishkind, Y.L. Wang, Orientation and three-dimensional organization of
26 actin filaments in dividing cultured cells, *J. Cell Biol.* (1993).
27 <https://doi.org/10.1083/jcb.123.4.837>.
- 28 [40] N. Taneja, A.M. Fenix, L. Rathbun, B.A. Millis, M.J. Tyska, H. Hehnlly, D.T.
29 Burnette, Focal adhesions control cleavage furrow shape and spindle tilt during
30 mitosis, *Sci. Rep.* (2016). <https://doi.org/10.1038/srep29846>.

1

2

Journal Pre-proof

1 **Figure Legends**

2

3 **Fig. 1. Proteins involved in cytokinesis localize at the apical junctional**
 4 **complex.** (A) F-actin was detected with fluorescent phalloidin and myosin heavy
 5 chain A (MHCA) and anillin by indirect immunofluorescence with specific antibodies.
 6 DNA stained with TO-PRO-3 is shown in inset. Orthogonal projections along the
 7 dashed lines are shown below apical views. Arrowheads point to the concentration of
 8 the labelling at the apical and lateral junctions. (B) Orthogonal projections of cells
 9 labelled by indirect immunofluorescence of F-actin and β -catenin. DNA stained with
 10 TO-PRO-3 (grey) was merged with F-actin and β -catenin. Arrowheads point to the
 11 concentration of the labelling at the apical and lateral junctions. (C) Co-labelling by
 12 indirect immunofluorescence of Rock II and phosphorylated S19MRLC (pS19MRLC,
 13 activated myosin) with the adherens junctional protein C-cadherin. The confocal
 14 planes passing through the apical junctions and overlays are shown. Orthogonal
 15 projections along the dashed lines are shown. Arrowheads point to the concentration
 16 of the labelling at the apical junctions. Scale bars: 10 μ m.

17

18 **Fig. 2. Accumulation of cytokinetic proteins begins at the apical junctions and**
 19 **further spreads basally along the lateral plasma membrane.**

20 Lifeact-GFP (A), SF9-GFP (B), 3xGFP-anillin (C) and GFP-Rock II KR (D) were
 21 expressed in living embryos and imaged. For each fluorescent protein, the
 22 representative still images of a dividing cell are shown. Time 0 corresponds to the
 23 start of fluorescent protein accumulation at the apical cell-cell contacts (time is
 24 indicated in seconds). Black arrowheads indicate ring contraction onset at the basal
 25 side. White arrowheads points on the accumulation of fluorescent proteins at the
 26 contractile ring. Below: orthogonal projections of a single lateral cell-cell contact
 27 (indicated by a dotted circle in front views) from the onset of fluorescent protein
 28 accumulation to the onset of ring contraction. Histograms show relative fluorescence
 29 intensity vs cell-cell contacts length at the onset of fluorescent protein accumulation
 30 (blue) and at the onset of ring contraction (red). a. : apical, b. : basal. ***: p-values <
 31 0.001. Scale bars: 10 μ m. (E) Duration of cytokinetic proteins accumulation at the
 32 division site. The time between the onset of proteins accumulation and actomyosin

1 ring constriction was measured for the four fluorescent proteins. The number of cells
 2 analysed for Lifeact-GFP, SF9-GFP, 3xGFP-anillin and GFP-Rock II KR are
 3 respectively 11, 9, 17 and 11. Standard deviations are indicated.

4

5 **Fig. 3. Activation of the actomyosin contractile ring is polarized.**

6 Indirect immunofluorescence for Rock II (A) and pS19MRLC (D). Surface views (Z0)
 7 and confocal planes 10 and 5 μm below are shown for respectively Rock II and
 8 pS19MRLC. Inset shows DNA detected with TO-PRO-3. Cells in metaphase, early
 9 anaphase, cytokinesis onset and advanced cytokinesis are presented for each
 10 antibody used. Orthogonal projection along the dashed lines are shown below. The
 11 horizontal and vertical dashed lines (shown only for metaphase cells) indicate the
 12 plane used to obtain orthogonal projection, respectively at the division sites and at
 13 the poles. Histograms B and E show pixel intensity of respectively Rock II and
 14 pS19MRLC fluorescence at the division site (blue circles) and poles (orange circles).
 15 The positions where the fluorescence intensity was measured are marked by blue
 16 (division site) and orange (poles) arrowheads on orthogonal projections. $n= 50$ for
 17 Rock II and 45 for pS19MRLC. Histograms C and F show pixel intensity of
 18 respectively Rock II and pS19MRLC fluorescence at the division site (blue circles)
 19 and poles (orange circles) as a function of the length of the lateral cell-cell contact
 20 labelled for respectively Rock II and pS19MRLC. Equations of the linear regressions
 21 are specified in the top right corner. Scale bars: 10 μm .

22

23 **Fig. 4. Destabilization of the adherens junctions increases the duration of**
 24 **cytokinetic proteins accumulation but does not impact the polarity of**
 25 **cytokinetic proteins recruitment and asymmetric ring constriction.**

26 (A) Expression of the C-cadherin deletion mutant, Ctail, destabilizes adherens
 27 junctions. Embryos expressing GFP-gpi or RFP-gpi alone (control) and co-expressing
 28 Ctail with GFP-gpi or RFP-gpi used as tracers were fixed and processed for indirect
 29 immunofluorescence with antibodies against C-cadherin, α and β -catenins and Rock
 30 II or with fluorescent phalloidin (to detect F-actin). GFP-gpi and RFP-gpi tracers were
 31 detected by immunofluorescence with antibodies against GFP and RFP, respectively.
 32 Apical confocal planes and orthogonal projections are shown. DNA is shown on

1 merge images. Histograms represent the relative pixel intensity of each protein in
 2 control and Ctail expressing cells. ***: p-values <0.001. Scale bar: 10 μ m.
 3 (B and D) Effect of Ctail expression on the duration of Lifeact-GFP (B) and 3xGFP-
 4 anillin (D) accumulation at apical cell-cell contacts. (B) Upper images show
 5 kymographs of orthogonal projections of one lateral plasma membrane at the division
 6 site of cells co-expressing lifeact-GFP alone (control) and Lifeact-GFP and Ctail
 7 (Ctail). Images are from the onset of fluorescent protein accumulation to the onset of
 8 ring constriction. a. : apical, b. : basal. Below, images are orthogonal projections of
 9 the plasma membrane at the division site of cells co-expressing Lifeact-GFP alone
 10 (control) and Lifeact-GFP with Ctail (Ctail) from the cytokinesis onset to the beginning
 11 of actomyosin ring constriction. (C) Histograms represent the time between the onset
 12 of proteins accumulation and actomyosin ring constriction for Lifeact-GFP alone
 13 (grey, n=11) and Lifeact-GFP and Ctail (brown, n=15). The p-value is indicated.
 14 (D and E) Same as in B and C with 3xGFP-Anillin. n=17 and 11 for respectively
 15 3xGFP-anillin alone and 3xGFP-anillin with Ctail.

16

17 **Fig. 5. Depletion of α catenin increases the duration of ring formation.**

18 (A) Endogenous α catenin and C-cadherin in embryos injected with α -catenin
 19 morpholino and RFP-membrane mRNA used as a tracer. For each condition, an
 20 image of a field containing cells expressing and not expressing RFP-membrane
 21 (asterisks) is shown. Red and blue bars on merged images indicate cell-cell contacts
 22 where fluorescence was quantified. Cells that do not express RFP-membrane are
 23 used as an internal control for fluorescence quantification. Line scans on the right
 24 show α -catenin and C-cadherin pixel intensity in internal control (blue) and cells
 25 expressing the RFP-membrane. Scale bars: 10 μ m.

26 (B) Kymograph of a baso-lateral plasma membrane at the site of division of a cell
 27 expressing Lifeact-GFP in control or α catenin morpholino. Histogram is the time of
 28 Lifeact-GFP accumulation in control or α -catenin morpholino (n=12 and 24 for
 29 respectively control and α catenin morpholinos). The p-value is indicated.

30 (C) Same as in B with 3xGFP-Anillin instead of Lifeact-GFP. (n=9 and 19 for
 31 respectively control and α catenin morpholinos)

32 (D) Schematic representation of cytokinesis initiation in polarized epithelial cells. The
 33 mitotic furrow, which is asymmetrically positioned along the apicobasal axis, signals

- 1 the position of the contractile ring to the apical cell-cell contacts. This leads to
- 2 extremely rapid ring formation spreading laterally from apical contacts towards the
- 3 basal side of cells.
- 4

Journal Pre-proof

1 **Supplementary figure legends**

2

3 **Fig. S1.** (related to Fig. 1): MKLP1 and ECT2 were detected with specific antibodies
4 in fixed embryos.

5 (A and C) Surface views and orthogonal projections of cells in interphase are shown
6 for each protein. Arrowheads point to the concentration of the labelling at the apical
7 junctions.

8 (B and D) Surface views and orthogonal projections of cells in anaphase are shown
9 for each protein. Orthogonal projections along the equatorial axis (horizontal) and
10 along the axis passing by the cell poles (vertical) are shown. Black arrowheads point
11 to the concentration of the labelling at the apical and lateral junctions. Scale bars: 10
12 μm .

13

14 **Fig. S2.** (related to Fig. 2):

15 (A) The four fluorescent proteins Lifeact-GFP (a probe for F-actin), SF9-GFP (a
16 probe for Myosin Heavy Chain), 3xGFP-anillin and GFP-Rock II KR localize at apical
17 cell junctions in interphase cells. Representative surface views are presented. Below,
18 orthogonal views are shown. White dotted lines on surface images symbolize the
19 plan of orthogonal projection. Arrowheads indicate apical accumulation of fluorescent
20 proteins.

21 (B) The duration of the actomyosin ring constriction is not significantly modified by
22 expression of indicated fluorescent cytokinetic proteins compared with GFP-GPI..

23 The number of dividing cells analysed were 15, 16, 19, 17 and 17 for GFP-GPI,
24 Lifeact-GFP, SF9-GFP, 3GFP-anillin and GFP-Rock II K/R, respectively. Statistical
25 comparison between GFP-GPI and each fluorescent protein was made; p values are
26 indicated on bars.

27 (C) Still images of a representative division of a cell expressing 3xGFP-anillin. Apical
28 views are shown. Below, orthogonal projections through the plan parallel to the
29 division site indicated by a dotted line. Times are indicated in seconds. Scale bars: 10
30 μm .

31

32 **Fig. S3.** (related to Fig. 2): Still images of cells expressing GFP-GPI alone (A) and
33 ZO1-GFP co-expressed with RFP-GPI (B). In panel B, images corresponding to a
34 confocal plane at the level of tight junctions marked by ZO-1, and a confocal plane 15

1 μm below tight junctions are presented. Time 0 corresponds to the onset of
2 actomyosin ring constriction at the basal side. Below surface views, orthogonal
3 projections through the axis indicated by dashed lines passing by the division site.
4 Scale bars: 10 μm .

5

6 **Fig. S4.** (Related to Fig. 2): Apicobasal position of the mitotic spindle. Embryos were
7 fixed and processed for indirect immunofluorescence to detect the mitotic spindle,
8 cell-cell contacts and chromosomal DNA (red). Top images: confocal plane passing
9 by the mitotic spindle poles. An orthogonal projection along the dashed line in top
10 image is shown below. White arrows point on the spindle poles. The mean values for
11 cell height and the distance of the mitotic spindle from apical and basal surfaces of
12 cells are indicated ($\pm\text{SEM}$, $n = 20$ spindles in 2 embryos). Scale bar: 10 μm .

13

14 **Fig. S5.** (related to Fig. 3): (A) Still images of cells expressing the GFP-rGBD probe
15 at a subapical confocal plane (Z_0), 2 μm and 4,5 μm below. The upper panel show
16 cells expressing high levels of GFP-rGBD (and consequently highly fluorescent) while
17 the lower panel shows cells expressing lower levels of GFP-rGBD. Arrowheads point
18 on GFP-rGBD localised at the cell equator when ring constriction is already
19 advanced. GFP-rGBD enrichment at the cell equator is absent in early cytokinesis.
20 These cells are representative of 16 analysed cells. (B) Validation of anti-
21 phosphoS19MRLC antibodies. Embryos were fixed and treated with phosphatase
22 buffer without (left) and with phosphatase (right). 3 confocal planes are presented.
23 The orthogonal projections through the axis passing by the division site indicated by
24 dashed lines on the front view are shown for each condition. Scale bars: 10 μm .

25

26 **Fig. S6.** (related to Fig. 4): Tight junctions are unaffected by Ctail. Embryos
27 expressing RFP-gpi alone (control) and co-expressing Ctail with RFP-gpi
28 (membrane) used as a tracer were fixed and processed for indirect
29 immunofluorescence with antibodies against the tight junction proteins ZO-1 and
30 occludin. Apical confocal planes and orthogonal projections are shown. DNA is
31 shown on merge images. Histograms represent the relative pixel intensity of each
32 proteins in control and Ctail expressing cells. n.s.: not significant. Scale bars: 10 μm .

33

- 1 **Fig. S7.** (related to Fig. 5): Cells expressing 3xGFP-anillin in control or α -catenin and
- 2 ZO-1 morpholinos. For each condition, still images of a representative dividing cell
- 3 are shown. Apical views are shown. Below, orthogonal projections through the plan
- 4 parallel to the division site indicated by a dotted line. Times are indicated in seconds.
- 5 Scale bars: 10 μm .

Journal Pre-proof

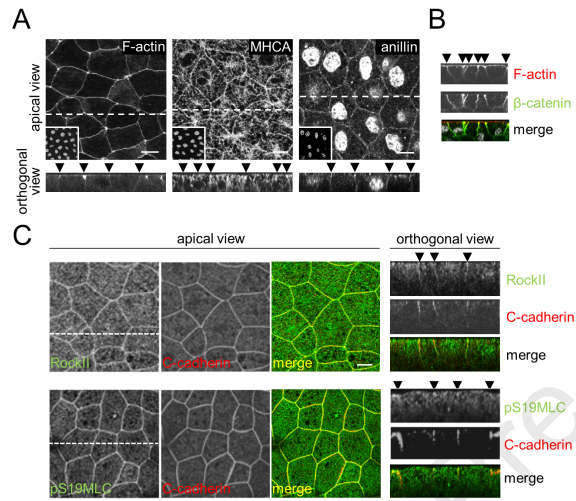


Figure 1

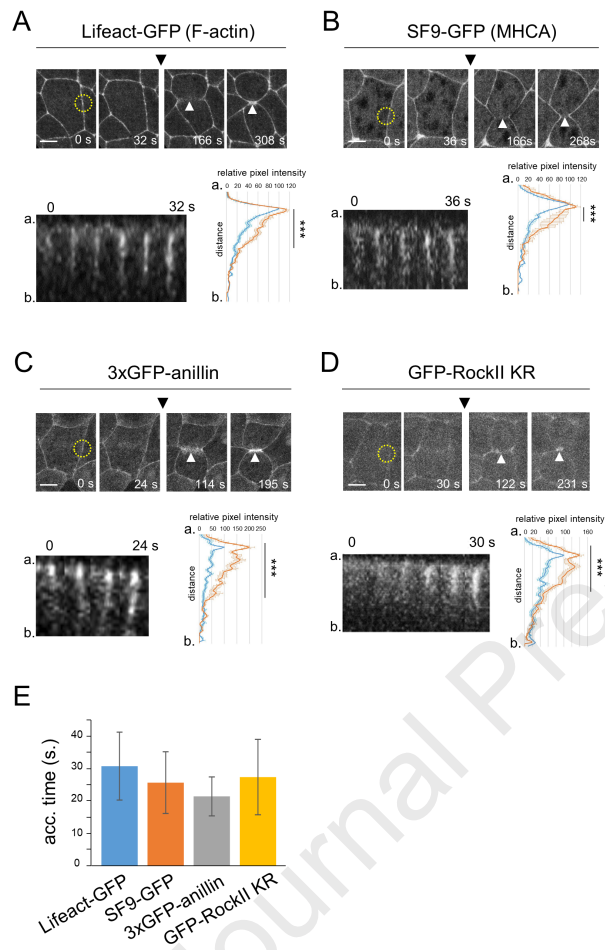


Figure 2

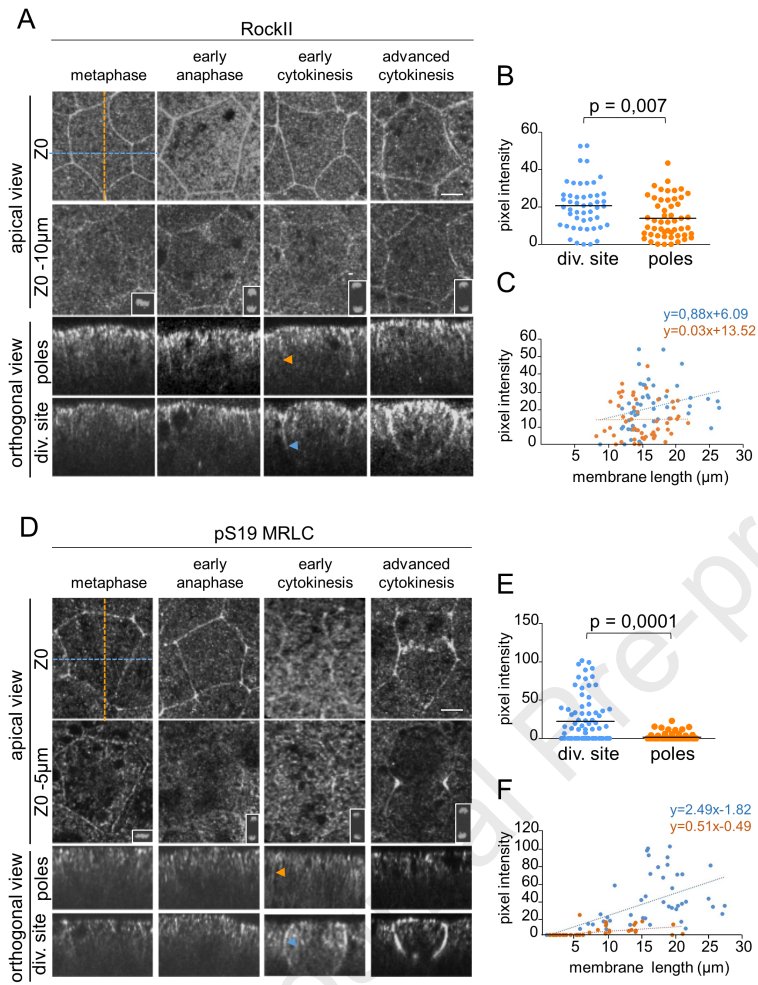


Figure 3

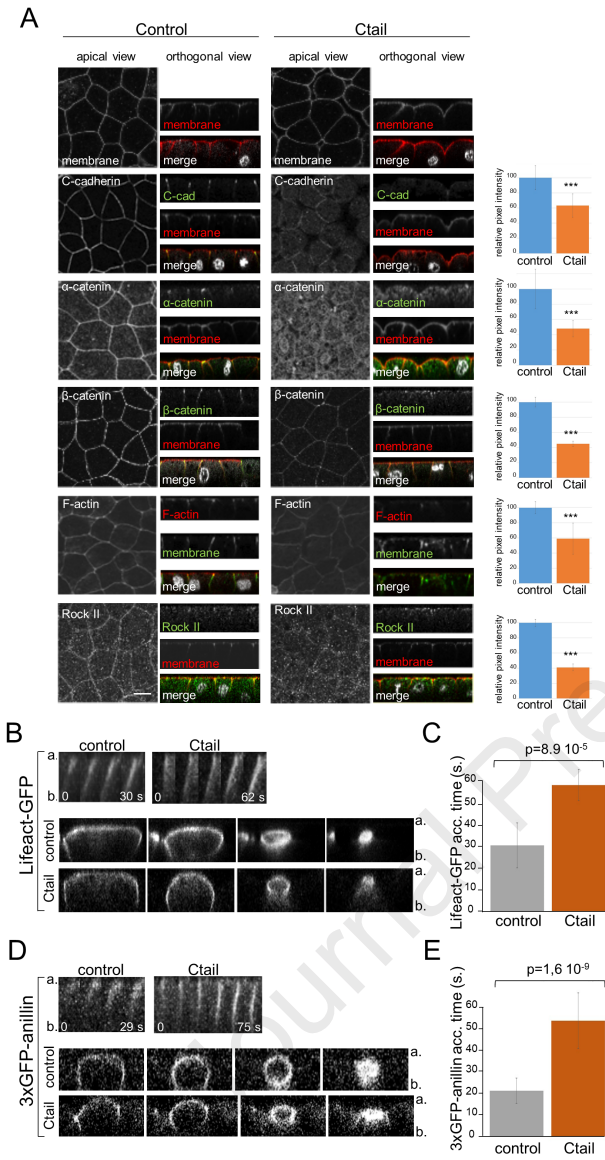


Figure 4

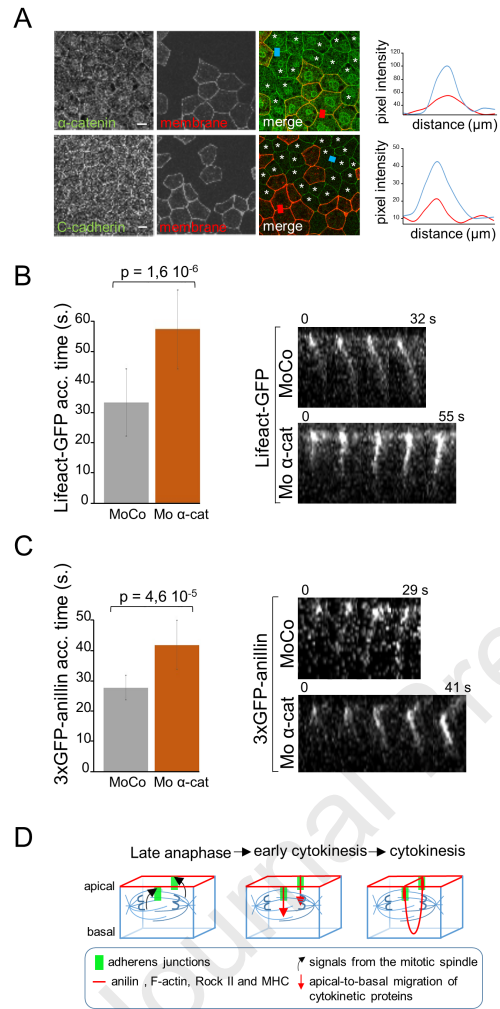


Figure 5

Highlights :

- The actomyosin contractile ring formation is polarised in epithelial cells
- Activation of the contractile ring is polarized in epithelial cells
- Adherens junctions are involved in the kinetics of the contractile ring formation
- Adherens junctions and the contractile ring are linked from the onset of cytokinesis
- High temporal resolution microscopy of epithelial cells in the *Xenopus* embryos

Journal Pre-proof

Conflict of interest

The authors declare no conflict of interest.

Journal Pre-proof